

Electrochemiluminescence Detection of Silver Ion Based on Trigeminal Structure of DNA

Zhejian Li,¹*^a Xuemei Fan,^a Baoyue Cao,^a Fei Yuan,^a Fengying Chen^a and Shumin Wang*^a

^aCollege of Chemical Engineering and Modern Materials, Shangluo University,
726000 Shangluo, P. R. China

A novel electrochemiluminescence (ECL) biosensor for highly sensitive and selective detection of Ag⁺ is developed based on the sensitive “turn-on” structure-switching trigeminal structure of deoxyribonucleic acid (DNA-TS). DNA-TS consists of three oligonucleotides hybridized to form three double-stranded DNA like Y-shaped DNA structure. The formation of DNA-TS makes the ECL sign Ru(bpy)₂(mcbpy-O-Su-ester)(PF₆)₂ of reporter probe approach to the electrode surface and thus increase the ECL signal intensity. The “signal-on” ECL biosensor could detect Ag⁺ concentration in the range from 1.0 × 10⁻¹¹ to 3.2 × 10⁻⁹ mol L⁻¹, and the limit of detection is 3.0 × 10⁻¹² mol L⁻¹. The strategy is sensitive and rapid. This approach could be extended to the design of sensors for other desired heavy metal ions as well. Such ECL sensors are promising for sensitive detection of other heavy metal ions.

Keywords: electrochemiluminescence, sensor, silver-specific oligonucleotide, silver ion

Introduction

As one of the trace elements in the human body, silver ions (Ag⁺) are harmless in trace amounts. However, overuse of silver ion-containing compounds risks polluting the environment.¹ Excess silver ions could cause inactivation of thiol-containing enzymes through the Ag–S bond. Meanwhile, silver ions can also interact with amino acids, imidazole and carboxyl groups of various metabolites, thereby posing a threat to human health.^{2,3} As such, there has been increased interest in developing fast and convenient methods to detect Ag⁺ in real-time. Traditional Ag⁺ detection methods include plasma atomic emission spectrometry,⁴ atomic absorption spectrometry (AAS),⁵ fluorescence spectroscopy,⁶ ion selective electrodes (ISE),⁷ anodic stripping voltammetry,⁸ microprobes,⁹ etc. These conventional methods typically have poor selectivity or sensitivity, and require complicated pre-treatment of samples, as well as not being appropriate for point-of-use applications.^{10,11} Therefore, the development of simple methods for highly selective and sensitive determination of Ag⁺ in life sciences, environmental protection and other related research fields is still a great challenge.

The highly selective and unique strong C–Ag⁺–C interaction has made oligonucleotides a novel candidate for the detection of Ag⁺. For example, Ag⁺ can mediate

the interaction between two cytosine molecules to form stable C–Ag⁺–C base pairs.¹²⁻¹⁵ A series of Ag⁺ biosensors of very high selectivity have been developed on the basis of the interaction between Ag⁺ and specific deoxyribonucleic acid (DNA) scaffold.¹⁶⁻¹⁹ These methods are based on the mismatched structure of C–Ag⁺–C, and include fluorescence analysis,²⁰⁻²² colorimetric analysis,²³ electrochemical detection²⁴⁻²⁶ and optical quantification.²⁷ Electrochemiluminescence (electrogenerated chemiluminescence, abbreviated as ECL) is a combination of electrochemical and luminescence techniques.^{28,29} It has been proven to be a powerful analytical technique and used for the detection of compounds through coupling with molecular recognition materials, such as aptamers, DNA and antibodies.^{30,31}

Inspired by previous researches reported in literature,³²⁻³⁴ the present study utilized the trigeminal structure of DNA and C–Ag⁺–C base-pair formation to develop an ECL biosensor for Ag⁺ detection. The mechanism of the biosensor is shown in Figure 1. First, the pretreated Au electrode was modified with thiolated capture probe P1, and P1 self-assembled onto the Au electrode surface via Au–S affinity. Then 6-mercaptohexanol (MCH) was used to block the non-specific sites not occupied by P1. Lastly, a mixed solution of Ru(bpy)₂(mcbpy-O-Su-ester)(PF₆)₂ (Ru1) labeled probe P2, auxiliary probe P3, and Ag⁺ was deposited onto the modified electrode, where the mismatched pairing of C–Ag⁺–C, induced by Ag⁺, caused the DNA chains of P1,

*e-mail: zhejian2621@163.com; 422686504@qq.com

P2 and P3 to form a trigeminal structure of DNA, which makes the ECL sign Ru1 of reporter probe approach to the electrode surface and thus increase the ECL signal intensity. This method for the detection of Ag^+ is precise, sensitive, fast, easy and high selective. To the best of our knowledge we, for the first time, report the ECL detection of Ag^+ using the highly selective cytosine- Ag^+ -cytosine coordination and the sensitive “signal-on” trigeminal structure of DNA.

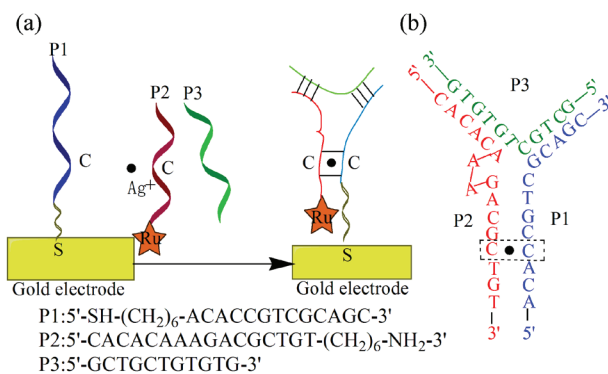


Figure 1. Schematic representation of (a) the designed electrogenerated chemiluminescence biosensor for Ag^+ and (b) the single C- Ag^+ -C coordination induced synergy-dependent trigeminal DNA structure.

Experimental

Reagents and instruments

6-Mercapto-1-hexanol (MCH) and $\text{Ru}(\text{bpy})_2(\text{mcbpy-O-Su-ester})(\text{PF}_6)_2$ (abbreviated as Ru1) were obtained from Sigma-Aldrich (USA). Oligonucleotides were synthesized and purified with polyacrylamide gel electrophoresis (PAGE) by Shanghai Sangon Biological Engineering Technology & Services Co., Ltd. (China). Their sequences are listed as: capture probe (5'-SH-(CH₂)₆-ACACCGTCGCAGC-3'), reporter probe (5'-CACACAAAGACGCTGT-(CH₂)₆-NH₂-3') and auxiliary probe (5'-GCTGCTGTGTG-3').

N,N-Dimethylformamide (DMF), anhydrous ethanol and tri-*n*-propylamine (TPrA) were purchased from the Xi'an Chemical Reagent Factory (China). All other reagents (analytical grades) were purchased from Sinopharm Chemical Reagent Co., Ltd. (China). Water used in this study was double deionized ultrapure water (Milli-Q 18.2 M Ω cm). DNA buffer (0.1 mol L⁻¹ NaCl in 10 mmol L⁻¹ Tris-HCl, pH 7.4) was used to dissolve and preserve DNA.

The device for ECL measurement consisted of a CHI600B Workstation (Shanghai CH Instruments, Inc., China) and an Ultra-Sensitive Luminescence Analyzer (Institute of Biophysics, Chinese Academy of Sciences,

China) with a traditional three-electrode system. The three-electrode system consisted of a fabricated sensor or a gold electrode (diameter (ϕ) = 2.0 mm) with modifications as the experimental electrode, a platinum wire as the counter electrode, and an Ag/AgCl electrode (in saturated KCl solution) as the reference electrode. The UV-Vis spectrum in this study was obtained on a UV-2450 UV-Vis spectrometer (Shimadzu Co., Japan). Fluorescence images were obtained with an Olympus IX-51 inverted microscope (Olympus Corporation, Japan) that was equipped with a mercury lamp (Olympus, Japan) and Olympus Dual CCD DP80 camera.

Synthesis of reporter probe

Briefly, 200 μL (2 OD (optical density), about 66 μg) of 3' NH_2 -oligonucleotides was added into 200 μL of Ru1 (1.0 $\times 10^{-3}$ mol L⁻¹, dissolved in DMF) and incubated with agitation at room temperature for 12 h. The above mixture was then added to 3.0 mL of anhydrous ethanol and 100 μL solution of sodium acetate (3 mol L⁻¹) and then cooled at -16 $^\circ\text{C}$ for 24 h. The solution was then centrifuged at 12000 rpm min⁻¹ for 30 min with refrigeration. The precipitate was washed with 2 mL of cold ethanol several times to remove unbound Ru1. The Ru1-labeled oligonucleotide probes were dissolved in 1.0 mL of 0.10 mol L⁻¹ phosphate-buffered saline (PBS), and stored at -16 $^\circ\text{C}$ until usage.

Preparation of ECL biosensor

Prior to each measurement, the Au electrodes were first cleaned by immersing them in piranha solution (30% H₂O₂:concentrated H₂SO₄, 1:3 v/v) for 2 h and then rinsed with Milli-Q water. Subsequently, the Au electrodes were polished with 0.03 μm Al₂O₃ slurry, followed by sonication with Milli-Q water, ethanol and Milli-Q water for 3 min in each, to rinse off any residual Al₂O₃ powder. The Au-electrode was then electrochemically cleaned in a 0.1 mol L⁻¹ H₂SO₄ solution by potential scanning within the potential range of -0.2 to 1.5 V until a reproducible voltammogram of gold was obtained. The electrode was then washed with water then blown dry with nitrogen.

Next, 6 μL of solution containing 0.5 $\mu\text{mol L}^{-1}$ capture probe was dropped onto the pretreated Au electrode and incubated for 4 h. The probe was washed twice with 0.1 mol L⁻¹ PBS solution to remove unbound capture probe. To reduce non-specific adsorption, the modified electrode was incubated in 1 $\mu\text{mol L}^{-1}$ 6-mercaptoethanol for 1 h so the capture probe could form a single-direction monolayer on the surface of the electrode.

ECL measurements

6.0 μL of mixture solution containing 1.0 $\mu\text{mol L}^{-1}$ of reporter probe, 1 $\mu\text{mol L}^{-1}$ of auxiliary probe and different concentrations of Ag^+ , was dropped onto the biosensor and incubated for 35 min, followed by 3 washes with the washing buffer. The biosensor treated with Ag^+ was then used as the working electrode in the ECL cell containing 3.0 mL of 0.10 mol L^{-1} TPrA-10 mmol L^{-1} PBS (pH 7.4) solution. The ECL measurement was performed with a scanning rate of 50 mV s^{-1} and a range of 0-1.4 V. The Ag^+ concentrations were quantified based on the ECL peak intensity change, $\Delta I = I - I_0$, where I_0 and I were ECL peak intensity before and after the ECL biosensing system interacts with Ag^+ , respectively. ECL detection and electrochemical impedance spectroscopy (EIS) measurements were both conducted in saturated and still air at ambient temperature.

Results and Discussion

Characteristics of the reporter probe

The reporter probe was characterized by UV-Vis absorption spectrophotometry and the fluorescence imaging. Figure 2A shows the UV-Vis spectrum of probe DNA (P2), Ru1 and reporter probe (P2-Ru1). A characteristic DNA peak was observed at 260 nm for the probe DNA in Figure 2a. Three characteristic peaks were observed between 220 and 500 nm for Ru1 in Figure 2b. The UV-Vis spectrum of the reporter probe was shown in Figure 2c, where the characteristic peaks at 278 and 258 nm corresponded to the absorption of Ru1 at 287 and 260 nm, respectively, with slight shift towards blue light. The absorption of the reporter probe at 460 nm was characteristic of absorption of the metallic ruthenium, which indicates conjugation of Ru1 into the DNA P2.

The reporter probe concentration was calculated to be 1.3×10^{-6} mol L^{-1} on the basis of the UV-Vis spectra. Figure 2B shows the fluorescence imaging of the reporter probe. These manifested that the ECL signal substance Ru1 had been coupled with the DNA P2.

Characteristics of the electrode assembling process

EIS was verified to be a powerful technique to determine the fabrication of the sensing interface and binding process.³⁵ To investigate the surface interactions, EIS measurements were tested. Figure 3 displays the impedance spectra in the form of a Nyquist plot obtained at the different electrodes. The fabrication of the sensing interface and binding process were subjected to the step-by-step modification process. The electron transfer resistance (R_{et}) at the bare Au electrode was about 145.91 Ω (Figure 3, curve a). This is attributed to that the bare gold electrode is an ideal conductor. After thiolated P1 self-assembled on the Au electrode surface, the R_{et} value increased to 1659.6 Ω (Figure 3, curve b), which indicated successful fixation of the P1 chain onto the Au electrode. After blocking with 1 mmol L^{-1} MCH, the R_{et} value increased to 4513.7 Ω (Figure 3, curve c), which is caused by the blocking of the residual sites on the electrode surface by the thiol bonds in MCH, and further reduction of the transmission of $[\text{Fe}(\text{CN})_6]^{3-/4-}$ on the electrode surface. After further reaction with 6 μL mixture solution including 1.0 $\mu\text{mol L}^{-1}$ P2/P3 and 1 mmol L^{-1} Ag^+ for 60 min, the R_{et} of the biosensor increased further, with the R_{et} value increasing from 4513.7 to 10206 Ω (Figure 3, curve d). This is mainly due to the negative charge of DNA phosphate backbone, which can repel negative charged $[\text{Fe}(\text{CN})_6]^{3-/4-}$, preventing $[\text{Fe}(\text{CN})_6]^{3-/4-}$ from reaching the electrode surface and therefore increasing the electrode impedance. All the above results indicated successful preparation of the ECL biosensor.

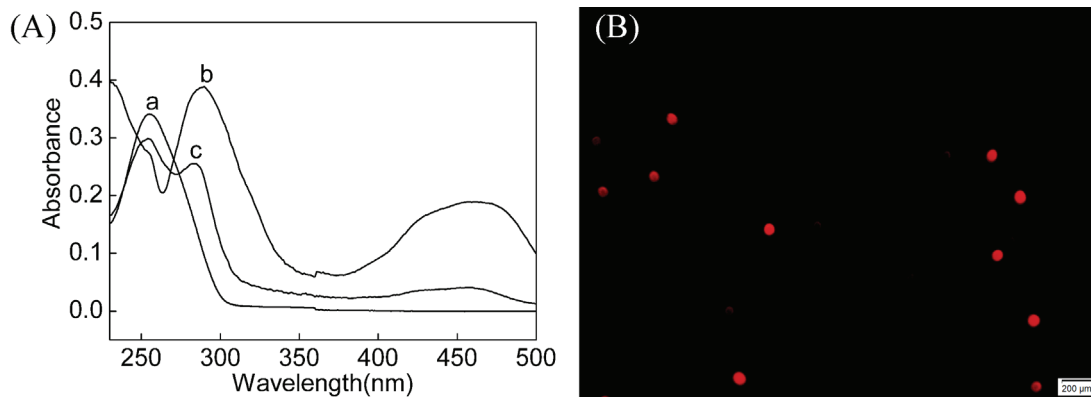


Figure 2. (A) UV-Vis absorption spectra and (B) fluorescence CCD imaging of the reporter probe. (a) 10.0 $\mu\text{mol L}^{-1}$ P2; (b) 9.0 $\mu\text{mol L}^{-1}$ Ru1 and (c) 1.3 $\mu\text{mol L}^{-1}$ reporter probe.

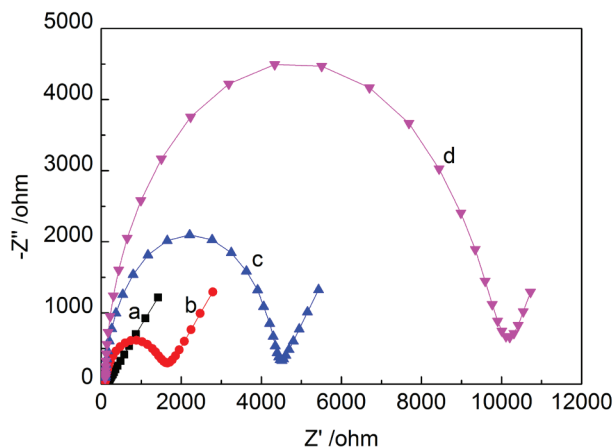


Figure 3. Nyquist diagram for the Faradaic impedance obtained at different electrodes in $5.0 \text{ mmol L}^{-1} [\text{Fe}(\text{CN})_6]^{3-/4-}$ solution (containing $10 \text{ mmol L}^{-1} \text{ KCl}$) with a scanning rate of 50 mV s^{-1} in the frequency range from 100 kHz to 0.1 Hz . (a) Bare gold electrode; (b) P1/gold electrode; (c) P1/MCH/gold electrode; (d) P3/P2/P1/MCH/gold electrode after interaction with $1 \text{ nmol L}^{-1} \text{ Ag}^+$.

Feasibility of detecting Ag^+ through ECL measurement

Figure 4 shows the ECL intensity changes before and after the ECL biosensor reacted with 3.2×10^{-10} or $3.2 \times 10^{-9} \text{ mol L}^{-1} \text{ Ag}^+$ solution, respectively. The ECL peak values after the sensor reacted with Ag^+ of 3.2×10^{-10} and $3.2 \times 10^{-9} \text{ mol L}^{-1}$ were 7605 (Figure 4, curve b) and 14011 (Figure 4, curve c), respectively, indicating that detection of Ag^+ with the developed ECL sensor was feasible.

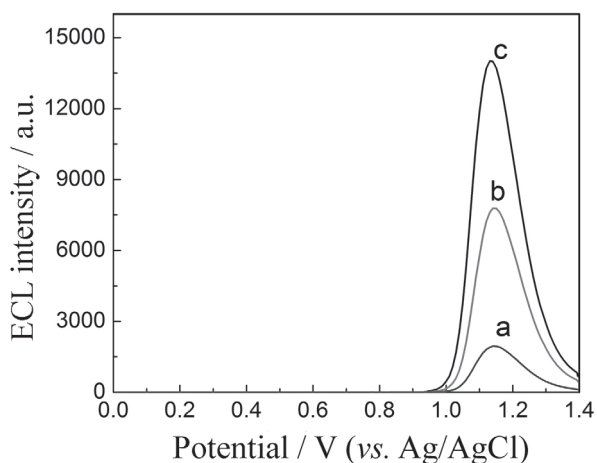


Figure 4. ECL intensity-potential profiles of the ECL biosensors before (line a) and after interaction with $3.2 \times 10^{-10} \text{ mol L}^{-1}$ (line b) and $3.2 \times 10^{-9} \text{ mol L}^{-1} \text{ Ag}^+$ (line c). The ECL measurement was performed in the ECL cell containing 3.0 mL of $0.10 \text{ mol L}^{-1} \text{ TPrA}$ - $10 \text{ mmol L}^{-1} \text{ PBS}$ ($\text{pH } 7.4$) solution with a scanning rate of 50 mV s^{-1} and a range of 0 - 1.4 V .

Optimization of experimental conditions

Optimization of the auxiliary probe concentration is shown in Figure 5a. The concentration of the target Ag^+

solution was $1.0 \times 10^{-9} \text{ mol L}^{-1}$, with a fixed mixture probe hybridization time of 40 min . DNA probes P2 and P3 were mixed at the same concentration and the concentration of auxiliary probes was changed in the range from 0 to $1.0 \text{ } \mu\text{mol L}^{-1}$ simultaneously, to investigate the effect of the concentration of auxiliary probe on ECL intensity. It should be noted that the concentration of the auxiliary probe had been maintained at the same level and were much higher than DNA P1 concentration. In Figure 5a, ECL intensity increased rapidly as the concentration of auxiliary probes increased within the range of 0 to $1.0 \text{ } \mu\text{mol L}^{-1}$. The increasing rate slowed down after the auxiliary probes reached $0.6 \text{ } \mu\text{mol L}^{-1}$. The ECL intensity hardly increased with increasing concentration of auxiliary probes after the concentration passed $1.0 \text{ } \mu\text{mol L}^{-1}$. The auxiliary probe concentration of $1.0 \text{ } \mu\text{mol L}^{-1}$ was therefore selected for all the following experiments in consideration of improving the sensitivity and saving reagent.

The relationship between the incubation duration of the biosensor with DNA probes P2, P3 and Ag^+ solution and the ECL intensity is shown in Figure 5b. When the incubation duration increased from 5 to 10 min , the ECL signal increased from 1200 to 4500 . When the incubation duration increased from 10 to 30 min , the ECL intensity kept increasing, plateauing at 9500 at the end. An

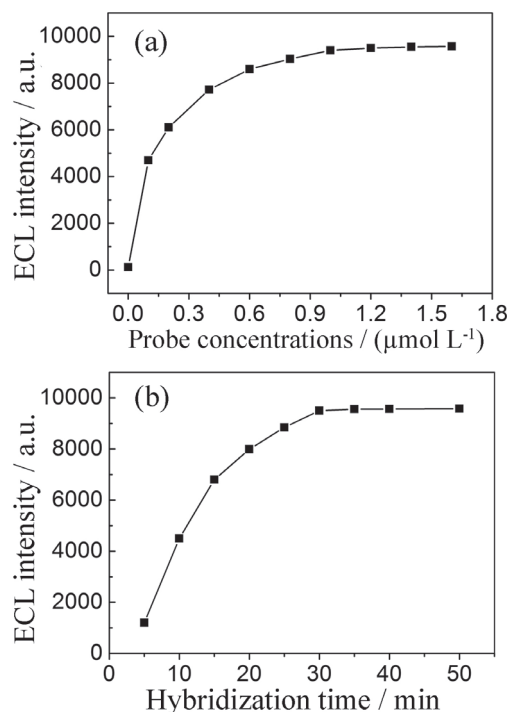


Figure 5. Effects of the concentration of auxiliary probes and binding time on the ECL intensity. (a) Dependence of the ECL intensity of the biosensor on the concentration of auxiliary probes; (b) dependence of the ECL intensity of biosensors on incubation time interaction with $1.0 \text{ nmol L}^{-1} \text{ Ag}^+$. The ECL measurement conditions were the same as in Figure 4.

incubation duration of 35 min was selected to ensure the reaction reached completion prior to measurement.

Performance of the biosensor for Ag⁺

Under the optimized conditions, the ECL signal intensity at different concentrations of Ag⁺ was determined. The response curve of ECL intensity and Ag⁺ concentrations is plotted in Figure 6. The peak height of the ECL signal increased in the presence of increasing Ag⁺ concentration, and the increased ECL peak intensity was directly linearly proportional to the logarithm of the Ag⁺ concentration within the range from 1.0×10^{-11} to 3.2×10^{-9} mol L⁻¹. The linear regression equation was $\Delta I = 3869.5 \log C$ (mol L⁻¹) + 44309.8, with a regression coefficient (R) of 0.9985. The limit of detection was 3.0×10^{-12} mol L⁻¹ Ag⁺ (defined as signal-to-noise (S/N) = 3), which was lower than those of the previous methods for Ag⁺ detection (Table 1). The low detection limit was attributed to the formation of trigeminal structure of DNA induced by a single C–Ag⁺–C base pair, which functions as a fixer to immobilize the Ru1 onto the electrode surface, increasing the chance of the Ru1 to collide with the electrode surface and facilitating the electron transfer.

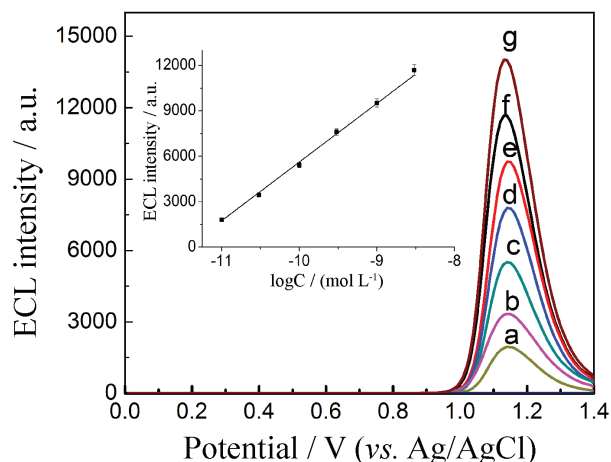


Figure 6. ECL intensity-potential profiles of the biosensor after interaction with various concentrations of Ag⁺ under the optimized conditions. (a) 0; (b) 10^{-11} ; (c) 3.2×10^{-11} ; (d) 10^{-10} ; (e) 3.2×10^{-10} ; (f) 10^{-9} ; (g) 3.2×10^{-9} mol L⁻¹. Insert: calibration curve of Ag⁺. The error bars represent the standard deviation of three repetitive measurements. The ECL measurement conditions were the same as in Figure 4.

The stability of sensor was also investigated. The sensor was stored at 4 °C for 20 and 30 days, respectively, and was used to measure 1.0 nmol L^{-1} Ag⁺ after each storage period. The ECL signal recoveries were 95.7 and 91.8%, respectively, indicating that the sensor developed in this study was stable over time under proper storage conditions.

Table 1. Comparison between previous studies and our proposed strategy

Method	Linear range / (mol L ⁻¹)	Limit of detection / (mol L ⁻¹)	Reference
EIS	0.1×10^{-9} to 100×10^{-6}	0.05×10^{-9}	24
EIS	10×10^{-12} to 100×10^{-9}	10×10^{-12}	36
SWV	2×10^{-9} to 100×10^{-9}	1.5×10^{-9}	37
SWV	0.5×10^{-9} to 1×10^{-3}	20×10^{-12}	26
DPV	10×10^{-9} to 500×10^{-9}	1.3×10^{-9}	38
DPV	1×10^{-12} to 100×10^{-9}	30×10^{-12}	39
Fluorescence	1×10^{-9} to 100×10^{-9}	1×10^{-9}	20
Fluorescence	20×10^{-9} to 150×10^{-9}	5.0×10^{-9}	21
SPR	50×10^{-9} to 2×10^{-6}	10×10^{-9}	40
ECL	10×10^{-12} to 3.2×10^{-9}	3.0×10^{-12}	this work

EIS: electrochemical impedance spectroscopy; SWV: square wave voltammetry; DPV: differential pulse voltammetry; SPR: surface plasmon resonance; ECL: electrochemiluminescence.

The selectivity of the biosensor was investigated by hybridization with 1.0 nmol L^{-1} of Ag⁺ and $1 \text{ } \mu\text{mol L}^{-1}$ of Cu²⁺, Zn²⁺, Cd²⁺, Pb²⁺, Fe²⁺, Co²⁺, Ca²⁺ and Ba²⁺, respectively. It was shown that the biosensor showed a remarkable response to 1.0 nmol L^{-1} Ag⁺, and the ΔI value in the presence of $1.0 \text{ } \mu\text{mol L}^{-1}$ Cu²⁺, Ca²⁺, Pb²⁺, Ba²⁺, Fe²⁺, Co²⁺, Cd²⁺, Zn²⁺ and Cd²⁺ was similar to the background signal. The specific assembly of C–Ag⁺–C coordination led to high selectivity for the detection of Ag⁺. The result shows that the approach exhibits high selectivity for Ag⁺, which gives it potential for future use.

The application of the ECL sensor was investigated by measuring the recovery of spiked Ag⁺ in real water samples collected from Nanqin River from Shangluo, China. Then the water samples were filtered with $0.2 \text{ } \mu\text{m}$ filter membrane to remove the floating matter in the water. The Ag⁺ concentration in the river was estimated by the proposed ECL sensor using the standard addition method. The results (Table 2) showed that the sensor constructed can be used for the detection of Ag⁺ in real water samples.

Table 2. Detection of Ag⁺ in water sample (n = 3)

Sample	Found / (10^{-10} mol L ⁻¹)	Added / (10^{-10} mol L ⁻¹)	Total / (10^{-10} mol L ⁻¹)	Recovery / %
1	4.60	5.00	9.69	102
2	3.42	5.00	8.58	103
3	4.24	5.00	9.48	105

To investigate the regeneration of sensors, they were immersed in 100 nmol L^{-1} Na₂S solution for 15 min after

each usage. However, the ECL signal could not return to the baseline, which demonstrated that the regeneration ability of the ECL sensor proposed is not satisfactory. This is attributed to the fact that the process of applied potential broke Au–S bond between thiol of the capture probe and the gold surface. Covalent coupling method for the fabrication of the carbon electrode-based sensor could improve regeneration ability of a biosensor.⁴¹

Conclusions

In conclusion, a novel ECL biosensor for the detection of Ag⁺ in aqueous media has been designed. The proposed analysis system was developed for “one-step” detection of Ag⁺. The assay is based on the highly selective C–Ag⁺–C coordination and the sensitive “turn-on” structure-switching trigeminal structure of DNA (DNA-TS). The DNA-TS functioned as a fixer to immobilize signal ruthenium complex of the reporter probe to collide with the electrode for fast electron transfer and increase the ECL intensity. The biosensors with a DNA-TS have exhibited improved sensitivity. The proposed biosensor showed potential application in other ECL or electrochemical biosensors, and possibly be utilized in other analytical instruments to quantitatively detect other heavy metal ions, proteins and small biomolecules.

Acknowledgments

This project was supported by the National Natural Science Foundation of China (No. 21703134) and the Natural Science Basic Research Plan in Shaanxi Province of China (No. 2018JM2040; 2018JQ2039; 18JS034).

References

1. Navarro, E.; Piccapietra, F.; Wagner, B.; Marconi, F.; Kaegi, R.; Odzak, N.; *Environ. Sci. Technol.* **2008**, *42*, 8959.
2. Dean, W. B.; *Chemosphere* **2000**, *40*, 1335.
3. Wood, C. M.; Donald, M. D. M.; Walker, P.; Grosell, M.; Barimo, J. F.; Playle, R. C.; Walsh, P. J.; *Aquat. Toxicol.* **2004**, *70*, 137.
4. Singh, R. P.; Pambid, E. P.; *Analyst* **1990**, *115*, 301.
5. Ghaedi, M.; Shokrollahi, A.; Niknam, K.; Niknam, E.; Najibi, A.; Soylak, M.; *J. Hazard. Mater.* **2009**, *168*, 1022.
6. Li, T.; Shi, L. L.; Wang, E. K.; Dong, S. J.; *Chem. - Eur. J.* **2009**, *15*, 3347.
7. Veerakumar, P.; Veeramani, V.; Chen, S.; Madhu, R.; Liu, S.; *ACS Appl. Mater. Interfaces* **2016**, *8*, 1319.
8. Baldo, M. A.; Daniele, S.; Ciani, I.; Bragato, C.; Wang, J.; *Electroanalysis* **2004**, *16*, 360.
9. Arai, Y.; Lanzirotti, A.; Sutton, S.; Davis, J.; Sparks, D.; *Environ. Sci. Technol.* **2003**, *37*, 4083.
10. Lin, Y. H.; Tseng, W. L.; *Anal. Chem.* **2010**, *82*, 9194.
11. Wang, R.; Wang, W.; Ren, H.; Chae, J.; *Biosens. Bioelectron.* **2014**, *57*, 179.
12. Zhao, C.; Qu, K. G.; Song, Y. J.; Xu, C.; Ren, J. S.; Qu, X. G.; *Chem. - Eur. J.* **2010**, *16*, 8147.
13. Hung, H. C.; Cheng, C. W.; Wang, Y. Y.; Chen, Y. J.; Chung, W. S.; *Eur. J. Org. Chem.* **2009**, *36*, 6360.
14. Zheng, H.; Yan, M.; Fan, X. X.; Sun, D.; Yang, S. Y.; Yang, L. J.; Li, J. D.; Jiang, Y. B.; *Chem. Commun.* **2012**, *48*, 2243.
15. Lin, C. Y.; Yu, C. J.; Lin, Y. H.; Tseng, W. L.; *Anal. Chem.* **2010**, *82*, 6830.
16. Qing, Z.; He, X.; Wang, K.; Zou, Z.; Yang, X.; Huang, J.; Yan, G.; *Anal. Methods* **2012**, *4*, 3320.
17. Xiao, Y.; Wu, Z.; Wong, K. Y.; Liu, Z.; *Chem. Commun.* **2014**, *50*, 4849.
18. Park, S. S.; Lee, J. Y.; Park, H. G.; *Chem. Commun.* **2012**, *48*, 4549.
19. Zheng, Y.; Yang, C.; Yang, F.; Yang, X.; *Anal. Chem.* **2014**, *86*, 3849.
20. Yang, Q.; Li, F.; Huang, Y.; Xu, H.; Tang, L.; Wang, L.; Fan, C.; *Analyst* **2013**, *138*, 2057.
21. Wen, Y. Q.; Xing, F. F.; He, S. J.; Song, S. P.; Wang, L. H.; Long, Y. T.; Li, D. C.; Fan, H.; *Chem. Commun.* **2010**, *46*, 2596.
22. Lotfi, B.; Tarlani, A.; Moghaddam, P. A.; Aghayan, M. M.; Peyghan, A. A.; Muzart, J.; Zadmar, R.; *Biosens. Bioelectron.* **2017**, *90*, 290.
23. Lin, Y. H.; Tseng, W. L.; *Chem. Commun.* **2009**, *43*, 6619.
24. Liu, G. P.; Yuan, Y. L.; Wei, S. Q.; Zhang, D. J.; *Electroanalysis* **2014**, *26*, 2732.
25. Zhang, Y. L.; Li, H. Y.; Xie, J. L.; Chen, M.; Zhang, D. D.; Pang, P. F.; Wang, H. B.; *J. Electroanal. Chem.* **2017**, *785*, 117.
26. Kim, J. H.; Kim, K. B.; Park, J. S.; Min, N.; *Sens. Actuators, B* **2017**, *245*, 741.
27. Yu, B.; Huang, Y. Y.; Zhou, J.; Guo, T.; Guan, B. O.; *Talanta* **2017**, *165*, 245.
28. Cui, H.; Paolucci, F.; Sojic, N.; Xu, G. B.; *Anal. Bioanal. Chem.* **2016**, *408*, 7001.
29. Pur, M. R. K.; Hosseini, M.; Faridbod, F.; Ganjali, M. R.; Hosseinkhani, S.; *Sens. Actuators, B* **2018**, *257*, 87.
30. Salehnia, F.; Hosseini, M.; Ganjali, M. R.; *Anal. Methods* **2018**, *10*, 508.
31. Pur, M. R. K.; Hosseini, M.; Faridbod, F.; Ganjali, M. R.; *Microchim. Acta* **2017**, *184*, 3529.
32. LaBean, T. H.; Yan, H.; Kopatsch, J.; Liu, F.; Winfree, E.; Reif, J. H.; Seeman, N. C.; *J. Am. Chem. Soc.* **2000**, *122*, 1848.
33. Cui, L.; Wu, J.; Li, M. Q.; Ju, H. X.; *Electrochem. Commun.* **2015**, *59*, 77.
34. Murakami, T.; Sumaoka, J.; Komiyama, M.; *Nucleic Acids Res.* **2012**, *40*, e22.

35. Zhang, D.; Zhang, Y.; Zheng, L.; Zhan, Y.; He, L.; *Biosens. Bioelectron.* **2013**, *42*, 112.
36. Yang, Y. Q.; Zhang, S.; Kang, M. M.; He, L. H.; Zhao, J. H.; Zhang, H. Z.; *Anal. Biochem.* **2015**, *490*, 7.
37. Zhang, Z. P.; Yan, J.; *Sens. Actuators, B* **2014**, *202*, 1058.
38. Yan, G. P.; Wang, Y. H.; He, X. X.; Wang, K. M.; Su, J.; Chen, Z. F.; Qing, Z. H.; *Talanta* **2012**, *94*, 178.
39. Xu, G.; Wang, G. F.; He, X. P.; Zhu, Y. H.; Chen, L.; Zhang, X. J.; *Analyst* **2013**, *138*, 6900.
40. Chang, C. C.; Lin, S. H.; Wei, S. C.; Yu, C. S.; Lin, C. W.; *Anal. Bioanal. Chem.* **2012**, *402*, 2827.
41. Sun, B.; Qi, H. L.; Ma, F.; Gao, Q.; Zhang, C. X.; Miao, W. J.; *Anal. Chem.* **2010**, *82*, 5046.

Submitted: October 8, 2018

Published online: February 5, 2019